Spin-Peierls and spin-liquid phases of Kagomé quantum antiferromagnets

J. B. Marston and C. Zeng
Laboratory of Atomic and Solid State Physics, Cornell University, Ithaca, New York 14853-2501

The ground state of the spin-$\frac{1}{2}$ nearest-neighbor Heisenberg quantum antiferromagnet on the Kagomé lattice probably lacks spin order; therefore, conventional spin-wave analysis breaks down. To ascertain the ground state, we instead use a systematic $1/n$ expansion with SU(n) fermions. Two distinct states occur in the large-n limit, depending on the size of the biquadratic interaction $\tilde{J}$. When $\tilde{J}=0$, there are an infinite number of degenerate ground states consisting of disconnected dimers. At finite n, however, this degeneracy is broken by local resonance. In contrast, a globally resonating chiral spin-liquid phase with no spin-Peierls modulation is the likely large-n ground state at sufficiently large $\tilde{J}$. For intermediate values of $\tilde{J}$, a phase transition from the dimer state to the chiral phase occurs as the temperature increases. At a higher temperature, there is a second transition to a paramagnetic state. We comment on the possibility that these phases are experimentally realized by the nuclear magnetic moments of a second layer of ^{3}He atoms lying on a graphite surface.

Novel ground states of low-spin quantum antiferromagnets may arise on low-dimensional, highly frustrated lattices. If spin order is absent, the usual spin-wave expansion about the ordered state breaks down and other means must be employed to find the ground state. (By spin order we mean the existence of a local spin moment. Néel order on the square lattice is the simplest example of such order.) The spin-$\frac{1}{2}$ nearest-neighbor Heisenberg antiferromagnet on the two-dimensional Kagomé lattice exhibits these features: The small value of the spin, the low coordination number ($z=4$), and the frustrating interactions all work against the formation of spin order. Indeed, exact diagonalization studies of clusters of up to 21 sites suggest that the local spin moment vanishes.[1] However, it is difficult to extract the nature of the order (or lack thereof) that occurs in the thermodynamic limit from these studies. Here, we report on a different approach that relies on a systematic expansion in powers of $1/n$, where n labels a generalization of the physical SU(2) spin to an antisymmetric, self-conjugate, representation of the group SU(n). [Note that $n>2$ *does not* correspond to a higher-spin representation of SU(2).] This technique was previously applied to the square lattice Heisenberg antiferromagnet, but it is particularly well suited for the Kagomé problem because spin order never occurs in the exactly solvable large-n limit.[2] Though the expansion parameter is of order 1 for the real problem, our approach makes definite predictions about possible ordering and the phase diagram that can then be tested by other means.

Many different SU(n) generalizations of the spin-$\frac{1}{2}$ SU(2) antiferromagnet are possible on unfrustrated, bipartite lattices; however, those approaches based on Schwinger bosons require different representations of SU(n) on the two sublattices and therefore do not work on the Kagomé lattice. In contrast, the fermionic path-integral approach works on all lattices and we employ it here. Since this method was discussed in some detail in Ref. 2, we limit our discussion to key points. The nearest-neighbor Heisenberg spin-spin coupling $J\mathbf{S}_x\cdot\mathbf{S}_y$ is first written as a four-fermion interaction involving the SU(n) destruction and creation operators $c_{\mathbf{x}\alpha}$ and $c_{\mathbf{x}}^{\dagger\alpha}$, where $\mathbf{x}$ labels the lattice site and $\alpha=1,2,\ldots,n$ is the flavor index. It is then decomposed via a Hubbard–Stratonovich transformation by introducing complex fields $\chi_{\mathbf{xy}}$ that live on the links of the lattice. The phases of the $\chi_{\mathbf{xy}}$ fields transform as spatial gauge fields under local U(1) gauge transformations of the fermions, and the time component of the gauge field appears in the guise of a Lagrange multiplier field ($\phi_{\mathbf{x}}$) that enforces the local particle-number constraint ($n/2$ fermions live on each site, where n is an even integer). The large-n solution then corresponds to the problem of finding the saddle point of the following functional integral representation for the partition function:

$$Z=\int [d\chi][d\phi]\exp -nS_{\text{eff}}[\chi,\phi].$$

Here, the effective action is given by an integral over the Grassman fields:

$$\exp -nS_{\text{eff}}[\chi,\phi]=\int [dc^*][dc]\exp -S[\chi,\phi,c^*,c],$$

where the imaginary time action is

$$S[\chi,\phi,c^*,c]=\int d\tau\Big[\sum_{\mathbf{x}} c_{\mathbf{x}}^{*\alpha}\frac{\partial}{\partial\tau}c_{\mathbf{x}\alpha}+i\phi_{\mathbf{x}}\Big(c_{\mathbf{x}}^{*\alpha}c_{\mathbf{x}\alpha}-\frac{n}{2}\Big)+\sum_{\langle\mathbf{xy}\rangle}\Big(\frac{n}{J}\Big)|\chi_{\mathbf{xy}}|^2+(\chi_{\mathbf{xy}}c_{\mathbf{y}}^{*\alpha}c_{\mathbf{x}\alpha}+\text{H.c.})\Big].$$

The implicit sum over the repeated flavor index makes each term in the action of order n. By choice of gauge, $\phi_{\mathbf{x}}$ can be set to zero. The integration over the fermions can in principle be done exactly (since they appear only at quadratic order) and the problem of finding the correct saddle point reduces to one of determining the static configuration of the $\chi_{\mathbf{xy}}$ fields which minimizes the effective action. Clearly, $\chi_{\mathbf{xy}}$ functions as the order parameter. Since it is invariant under global SU(n) transformations, spin order is impossible in the large-n limit.

 0021-8979/91/085962-03$03.00 © 1991 American Institute of Physics

Downloaded 06 Dec 2002 to 128.148.60.17. Redistribution subject to AIP license or copyright, see http://ojps.aip.org/japo/japcr.jsp

In a remarkable paper,[3] Rokhsar proved that the best saddle-point configuration on almost all lattices consists of a dimer covering of the lattice. That is, $|\chi_{xy}|$ is nonzero (and equal to $\overline{\chi}=J/2$) on one and only one of the links attached to each site. Rokhsar's proof applies to the Kagomé lattice, and since the coordination number $z=4$, only $\frac{1}{4}$ of the links are nonzero in this phase. The dimerization corresponds to spin-Peierls modulation since only spins connected by a dimer are correlated via a singlet bond. There are, however, an infinite number of ways to lay down the dimers and all of these states are degenerate in the large-n limit.

To ascertain how $1/n$ corrections break this degeneracy, we follow Read and Sachdev[4] and expand the effective action for the χ_{xy} fields in fluctuations $\delta\chi_{xy}$ about any given dimer configuration $\overline{\chi}_{xy}$. The order $n(\delta\chi)^2$ contribution was calculated in Ref. 4 for the square lattice, but does not lift the dimer degeneracy on the Kagomé lattice. It merely corrects the free energy (which is order n) by a constant of order 1 since $\langle(\delta\chi)^2\rangle = O(1/n)$. The first term that removes some degeneracy occurs at order $n(\delta\chi)^3$ in the effective action expansion and involves hexagons that have dimers on three of the links and fluctuations on the remaining three links. Clearly, this term contributes to the total free energy only at second order [that is, $n^2\langle(\delta\chi)^6\rangle$] because the quadratic part of the effective action is invariant under $\delta\chi_{xy} \rightarrow -\delta\chi_{xy}$. Since it is second order, it always lowers the free energy (by an amount of order $1/n$). Indeed, the hexagon behaves like the benzene molecule: Both lower their energy through resonance. Other corrections to the free energy appear at order $1/n$, but are independent of the dimer configuration.

Thus, the $1/n$ term picks patterns which maximize the number of hexagons with three dimers. A simple counting argument now shows that the maximum fraction of such hexagons (we call them "perfect hexagons") is $\frac{1}{6}$. Let N_3, N_{3d}, N_6, and N_{6p} be, respectively, the number of triangles, triangles without a dimer which we call "defect triangles," hexagons, and perfect hexagons. It was shown in Ref. 5 that $N_{3d} = \frac{1}{4}N_3$ for any dimer covering. According to the observation that (1) exactly three defect triangles are attached to every perfect hexagon, and (2) none of six nearest hexagons around a perfect one can be perfect (and, consequently, no two perfect hexagons will share a common defect triangle), we have $3N_{6p} \leqslant N_{3d}$. Combining these observations and using $N_3 = 2N_6$, we obtain $N_{6p} \leqslant \frac{1}{6}N_6$.

Further constraints on the 12 second-nearest hexagons around a central perfect one reveal how to construct patterns with the maximum fraction. First of all, only six of these 12 hexagons are potential sites for another perfect hexagon. The six hexagons that are separated from the central perfect one by two triangles ("bow ties") cannot support a perfect hexagon because the site in the center of the bow tie will not be attached to a dimer. Second, if we link the center of the central perfect hexagon to the centers of the two next closest possible perfect ones by two straight lines, then the angle between lines has to be either 120° or 180°. These two local rules generate various patterns which we classify by the size of the respective unit cells. Note that

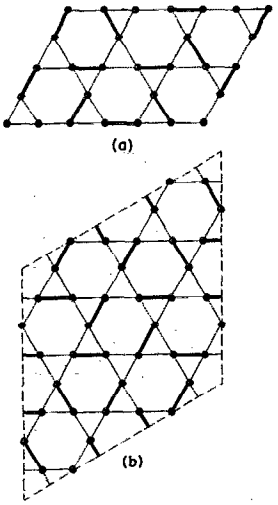

FIG. 1. Unit cells with the maximum fraction of perfect hexagons where the thick lines denote dimers. (a) 18-site unit cell with perfect hexagons that form a oblique lattice. (b) 36-site unit cell with perfect hexagons that form a honeycomb lattice.

configurations that differ by a rotation of the three dimers on a perfect hexagon by 60° are energetically equivalent at order $1/n$. We draw one of the several patterns for the smallest possible unit cell (18 sites) and one pattern fitting in the next smallest unit cell (36 sites) in Fig. 1.

Although we have not examined higher-order (beyond $1/n$) corrections, we fully expect these terms will break the remaining degeneracy and select out a phase with finite degeneracy. These terms involve increasingly large resonance patterns that eventually link the unit cells together. Thus, the dimers should solidify at zero temperature into a crystalline solid built out of unit cells constructed according to the above rules. Clearly, this long-range dimer order will melt at a nonzero temperature since the dimers do not break a continuous symmetry, but rather the discrete two-dimensional lattice translational symmetry.

As we mentioned earlier, there are actually many different SU(n) generalizations of our SU(2) Hamiltonian. Even in the context of our fermionic path-integral approach, we can add a nearest-neighbor biquadratic term to the Hamiltonian, without changing the physical SU(2) limit because $\tilde{J}(\mathbf{S}_x\cdot\mathbf{S}_y)^2 = -(\tilde{J}/2)\mathbf{S}_x\cdot\mathbf{S}_y + \text{const}$ for spin $\frac{1}{2}$. Clearly, adding the biquadratic interaction $\tilde{J}$ just amounts to a trivial renormalization of the usual bilinear spin-exchange constant J (at least if $\tilde{J}<2J$; otherwise, the system becomes a ferromagnet). But for $n>2$ this interaction represents new processes that simultaneously interchange two flavors of fermions on one site with two on another neighboring site. Thus, the inclusion of the biquadratic term furnishes us with a one-parameter family of SU(n) theories with the same SU(2) limit. For $\tilde{J}>0$ the bi-quadratic term frustrates spin-Peierls order because it favors states that spread out singlet correlations uniformly on all the links. Indeed, upon decomposing the biquadratic term via a two-stage Hubbard–Stratonovich transformation[2] (by introducing new real-valued link fields Φ_{xy}), we discover that "flux"-type states with uniform $|\chi_{xy}|$ are viable. (Bicubic, biquartic, and higher terms can also be included, but do not lead to any other new ground states.) If such a state persists down to $n=2$, then it realizes Anderson's resonating valence bonds (RVB) in the sense that

Downloaded 06 Dec 2002 to 128.148.60.17. Redistribution subject to AIP license or copyright, see http://ojps.aip.org/japo/japcr.jsp

each spin on a site participates equally in singlet correlations on all four links emanating from the site.

We study the crossover from the spin-Peierls phase to the globally resonating RVB states by integrating out the fermions in a number of different trial configurations of the χ_{xy} and Φ_{xy} fields. Since we are also interested in the effect of nonzero temperatures on the crossover, we compute the saddle-point free energy by using a Fermi–Dirac distribution for the fermion occupancy. The free energy per site (at temperature T and $J=1$) is

$$F(\chi,\Phi) = = 2an(|\chi|^2 - \Phi^2/\tilde{J}) - (n/2)b[\Omega_{xy};T].$$

Here, a denotes the fraction of links with nonzero $|\chi_{xy}|$; in this case, $a = \frac{1}{4}$ for the spin-Peierls phase and $a=1$ for the flux phases. Also, $\Omega_{xy} \equiv (1 + 2\Phi_{xy})^{1/2}\chi_{xy}$ and $b[\Omega_{xy};T]$ is the free energy at half-filling of the fermions that move from site to site along the nonzero Ω_{xy} links. We are assuming here that $|\chi_{xy}|$ and Φ_{xy} take on only two possible values on any given link: zero or a constant. We then must minimize F with respect to the χ_{xy} fields, but maximize it with respect to the Φ_{xy} fields (see Ref. 2).

The best RVB state ($a=1$) we found has a flux of $+\pi/2$ passing through the each triangle on the Kagomé lattice and zero flux in the hexagons. At zero temperature, this uniform flux phase drops below the spin-Peierls state in energy when $\tilde{J} > 0.92J$. It is clearly twofold degenerate because it breaks time-reversal symmetry (the state with flux $-\pi/2$ has the same energy). This state *does not* break translational or rotational symmetry, and it has no spin or spin-Peierls order. Rather, it is a chiral spin liquid: For SU(2) the expectation value $\langle \mathbf{S}_1 \cdot \mathbf{S}_2 \times \mathbf{S}_3 \rangle$ is nonzero and constant on every elementary triangle (with vertices at sites 1, 2, and 3). The fermion spectrum is completely gapped, and so we expect the spin-spin correlation function to exhibit exponential decay in the chiral phase.

The state with flux π through the hexagons and flux $\pi/2$ through the triangles and the state with no flux at all both have higher energy, regardless of the temperature. This result is in accord with heuristic rules found by Rokhsar.[6] He approaches the problem of finding the optimal flux states by first breaking up any lattice into its smallest closed polygons. He then notices that disconnected polygons with an odd number of sides (like the aforementioned triangles) prefer to have flux $\pi/2$ to minimize the fermion energy. Polygons with $4m$ sides, where m is an integer, want flux π, and finally polygons with $4m+2$ sides (the hexagons) prefer zero flux. Indeed, we may view the zero flux phase as an excited state of the chiral flux state with defect antiflux tubes passing through the triangles that cancel out the $\pi/2$ flux. Similarly, the phase with uniform $\pi/2$ flux in each triangle and π in the hexagons can be seen as an array of flux defects passing through the hexagons.

Rokhsar's rules do not distinguish between the state with uniform $\pi/2$ flux per triangle and the state with a staggered flux of $\pm\pi/2$. In fact, the uniform phase is energetically preferred. We gain some understanding of this fact by studying the Fermi surface of the staggered state with flux $+\pi/2$ in the upward pointing triangles and $-\pi/2$ in the downward ones. In the gauge in which only the horizontal links are imaginary ($\chi_{xy} = i|\chi|$ with the link orientation pointing either all to the left or all to the right), the Fermi surface (which is at zero energy because of particle-hole symmetry) has the shape of an isosceles triangle with vertices at momenta $(0, \pm\pi/\sqrt{3})$ and $(\pi,0)$. Apparently, the complete gap in the fermion spectrum of the uniform chiral phase forces the fermions into lower energy states than in the staggered phase. It also means that the uniform chiral phase is likely to be locally stable against $\delta\chi_{xy}$ perturbations at arbitrary wave vector.

If we choose $\tilde{J}$ to be slightly smaller than the critical value required to favor the chiral spin-liquid state over the spin-Peierls phase at zero temperature, then we find a first-order transition to the chiral liquid state at a nonzero temperature. For example, at $\tilde{J}=0.90J$ the transition occurs at a temperature of $T \approx 0.05J$. The liquid phase then survives up to $T=J/4$, where a second-order transition to a paramagnetic (gas) state marked by $|\chi_{xy}| = \Phi_{xy} = 0$ occurs. (A small-$|\chi|$ expansion of the free energy shows that this paramagnetic transition always occurs at $T=J/4$, regardless of the saddle point or the value of $\tilde{J}$.[7] Note that the entropy from different dimer configurations is of order 1, and so its contribution to the free energy can be neglected in the large-n limit.)

The above spin-Peierls solid to chiral liquid and chiral liquid to paramagnetic gas transitions may correspond to the two peaks in the specific heat seen in an exact diagonalization of a 12-site cluster[5] and an approximate decoupled-cell Monte Carlo calculation,[1] but further numerical work is needed to test for the existence of spin-Peierls or chiral order. In nature, the Kagomé system may be realized by a second layer of ^{3}He atoms adsorbed onto a graphite substrate at a particular coverage density.[5] The nuclear spins of the ^{3}He atoms interact via simple antiferromagnetic two-atom-exchange processes and ring exchanges involving more than two atoms, but the nearest-neighbor Heisenberg antiferromagnet may be a good starting point for further studies. In fact, experiments show at least one peak (entropy arguments suggest there are actually two peaks) in the specific heat at a temperature of about 2.5 mK.[8] It may be necessary to include other spin-exchange terms in a realistic model Hamiltonian,[9] and the methods developed here can easily be applied to more complicated systems that possess global spin-rotational symmetry.

We thank V. Elser, C. Henley, T. Hsu, and D. Rokhsar for helpful discussions. This work was supported by an IBM postdoctoral fellowship (J.B.M.) and NSF Grant No. DMR-88-18558 (C.Z.)

[1] C. Zeng and V. Elser, to appear in Phys. Rev. B **42**, 8436 (1990).
[2] J. B. Marston and I. Affleck, Phys. Rev. B **39**, 11,538 (1989).
[3] D. S. Rokhsar, Phys. Rev. B **42**, 2526 (1990).
[4] N. Read and S. Sachdev, Nucl. Phys. B **316**, 609 (1989).
[5] V. Elser, Phys. Rev. Lett. **62**, 2405 (1989).
[6] D. S. Rokhsar, Phys. Rev. Lett. **65**, 1506 (1990).
[7] J. B. Marston and D. S. Rokhsar (unpublished).
[8] D. S. Greywall and P. A. Busch, Phys. Rev. Lett. **62**, 1868 (1989).
[9] M. Roger, Phys. Rev. Lett. **64**, 297 (1990).

Downloaded 06 Dec 2002 to 128.148.60.17. Redistribution subject to AIP license or copyright, see http://ojps.aip.org/japo/japcr.jsp